Asian Journal of Chemistry; Vol. 37, No. 11 (2025), 2652-2660
ASIAN JOURNAL OF CHEMISTRY
https://doi.org/10.14233/ajchem.2025.34448

Theoretical and Experimental Studies of Non-Covalent Interactions in a Ternary Liquid Mixture of Toluene, DMSO and Butyl Acetate

PRATIBHA ARYA[1], TARA BHATT[2,*], LALIT MOHAN[3] and CHARU C. DHONDIYAL[1]

[1]Department of Physics, M.B.G. P.G. College, Haldwani Nainital-263139, India
[2]Department of Physics, L.B.S. Government P.G. College, Halduchaur, Nainital-263139, India
[3]Department of Chemistry, D.S.B. Campus, Kumaun University, Nainital-263001, India

*Corresponding author: E-mail: tarabhatttt@gmail.com

Received: 13 July 2025 *Accepted*: 30 August 2025 *Published online*: 27 October 2025 AJC-22151

The study investigates the nature and strength of forces responsible for the molecular association between pure liquids *viz*. toluene (Tol), dimethyl sulfoxide (DMSO) and butyl acetate (BA) as well as their ternary mixture, using spectroscopic and computational techniques. Quantum chemical calculations are done by using density function theory (DFT) in order to get the information regarding non-covalent interaction. Theoretical calculation of the interaction energies was conducted to understand the nature and strength of possible intermolecular interaction between the molecules. The optimized geometries of the monomers, their self-associated dimers and their complexes confirm the presence of CH-π, CH-C and OH bond in the ternary systems and are found to influence the interaction energies of the complexes. In addition to the theoretical study, UV-Vis absorption spectra of ternary liquid mixture at different mole fractions have been examined to investigate the nature of specific interactions. Further, the presence of non-covalent interactions and the strength of different type of molecular interaction, infrared spectra of a ternary liquid mixture of toluene, DMSO, butyl acetate at various concentrations at room temperature (20 ºC) have also been assessed through the change in the vibrational stretching frequency of various functional groups of pure liquids. The experimentally recorded UV-Vis spectra and the shift in the frequencies of the functional groups in FT-IR spectra are also supported by the theoretical quantum calculations.

Keywords: Intermolecular interaction, DFT, Toluene, Dimethyl sulfoxide, Butyl acetate.

INTRODUCTION

In recent years, mixed solvents are found to have immense practical applications in various chemical processes compared to pure solvents mainly due to their properties are less known [1,2]. The properties of liquids and their mixtures play a significant role in chemical engineering processes, simulations, solution theory in the textile industry and molecular dynamics [3]. These properties are used for studying the molecular interaction in pure liquids, liquid mixtures and the ionic interactions involved with both single and mixed solutes [4,5]. Liquid mixtures, due to their unique behaviour, have attracted considerable interest among the researchers [6]. Spectroscopic methods have emerged as powerful tools for studying the molecular dynamics of liquid mixtures, owing to their ability to characterize the physico-chemical properties of the liquid environment [8-10]. The study of liquid mixtures that contain both polar and non-polar components find valuable applications in polymer phase diagrams and the preferential interactions of polymers in mixed solvents [11] as well as in various industrial and technological applications [12].

Toluene, a non-polar aromatic hydrocarbon, is extensively used in the paint industry, adhesive manufacturing, leather tanning process and as a solvent for carbon nanomaterials. Dimethyl sulfoxide (DMSO), on the other hand, is a highly polar solvent (dipole moment = 3.96 D) [13]. It is also a strongly associated aprotic solvent due to its S=O group [14] and has multifunctional properties due to its two attached hydrophobic CH_3 groups. Therefore, it is worthwhile to investigate the molecular interaction of DMSO with non-polar aromatic hydrocarbons like toluene, which is essential for the understanding of various chemical and industrial processes. Much work is being reported on the mixture of toluene with other polar components [15-17]. The molecular interaction between the π-electron system of aromatic compounds and a hydrogen atom of alkanes (C-H/π interaction) is a significant topic of

interest in super molecular chemistry [18]. Typically, the C-H/π interaction is the interaction between a hydrogen atom of methane and an aromatic ring of toluene. The non-polar aromatic hydrocarbon has substantial quadrupole moment that induce an orientational order in esters. Butyl acetate, a moderately volatile polar solvent with a distinct ester odour, has wide range of applications in engineering, chemical and polymer process industries, as it is miscible with most common solvents. Moreover, due to its low water absorption, high resistance to hydrolysis and high solvency, butyl acetate can also serve as an extractant in pharmaceutical preparations and as an ingredient in cleaners, fragrances and essences. Other researchers [19-21] have also observed the participation of π electrons of toluene in hetero-molecular interactions. Therefore, it seems that the carbonyl oxygen of esters and the π-electrons of toluene play an important role in the molecular interactions within the liquid mixtures containing these substances.

The present investigation is based on the spectroscopic and theoretical methods to understand the molecular interactions in a ternary liquid mixture consisting of DMSO, toluene (an aromatic compound) and butyl acetate (an ester). To investigate the nature, sites of interactions, the degree of self-association among the molecules and the effects of mixing at different mole fractions, Fourier transform infrared (FT-IR) spectroscopy was used. This study also includes a method of analysis of intermolecular interactions in the ternary liquid mixture which is based on spectral data in the UV-Vis range. The quantum chemical investigations focused on the accurate prediction of molecular properties such as structure, stability and reactivity, as well as rationalizing and interpreting molecular properties based on simple models and concepts [22-25]. The DFT is used to optimize structures, calculate the bond parameters, dipole moments and interaction energies as it is computationally less costly and provides a better source of information regarding the non-bonded interactions [26-28].

EXPERIMENTAL

The chemicals of analytical reagent (AR) grade supplied by E. Merck Ltd. (India) with 99% purity were used without further purification. To prepare a mixture of various concentrations in mole fraction, a digital balance (Aczet Pvt. Ltd. India) was used with a precision of ± 1 mg. In all systems, the mole fraction of the second component, DMSO ($x_2 = 0.4$) was kept fixed while the mole fraction of the other two (x_1 of toluene and x_3 of butyl acetate) were varied from 0.0 to 0.6; to have the mixture of different composition. Varying the mole fraction of the second component around 0.4 does not lead to any significant changes in the observed properties. The FT-IR spectra were recorded in transmission mode for pure components and their mixtures at different concentrations. Samples were scanned using a Spectrum Two™ FT-IR spectrophotometer (Perkin-Elmer) equipped with a deuterated triglycine sulphate (DTGS) detector and KBr as a beam splitter. The instrument was connected to Spectrum 10 ES™ software and spectra were scanned at wave numbers of 4000-400 cm^{-1}, at a resolution of 2 cm^{-1} and room temperature 293 K. The UV visible absorption spectra of different compositions were recorded at room temperature by a Perkin-Elmer spectrophotometer (model Lambda-35) with a varying slit width in the range 190-900 nm. All optical measurements were performed under ambient conditions.

Computational analysis: To validate the experimental results, the geometrical structure, nature and interaction strength between the components, their dimers and complexes were evaluated and studied quantum chemically. In present work, the quantum chemical calculations were carried out using the Gaussian 09 programme [29]. The primary geometry of toluene (tol), dimethyl sulfoxide (DMSO) and butyl acetate (BA), their dimers and complexes were modeled with the help of the AVOGADRO programme [30]. The molecular geometry was further fully optimized in Gaussian and used as input for density functional theory (DFT). The well-known hybrid method B3LYP/6-31G(d,p) adopted in modern chemistry, is a combination of the Becke 3-parameter exchange functional, the Lee-Yang-Parr correlation functional (B3LYP) [31,32] and the 6-31G(d,p) basis set. The adopted basis set 6-31G(d,p) is widely used in Hartree Fock (HF) and MP2 calculations to produce satisfactory interaction energies, geometry and some hydrogen bonding energies [33]. Gauss view program used for visualization of the interaction between the components and post-processing of output data was done using CHEMCRAFT software [34].

RESULTS AND DISCUSSION

Quantum chemical studies

Molecular interaction: Molecular associations in a liquid mixture are due to inter/intramolecular packing through certain specific types of non-covalent interactions. Quantum mechanically optimized possible minimum energy structures of monomers are shown in Fig. 1 and self-assemblies (dimers) of pure liquids and their complexes obtained by GAUSSIAN are shown in Figs. 2a-g. The possible molecular interactions between the components obtained from structural changes are discussed as follows:

Tol-Tol: Toluene (Tol) is a methyl (-CH_3) carrying benzene ring in which the methyl group releases an electron through induction to the benzene moiety and enhances the π-electron density to the toluene ring. The π-ring (π-plane) and the attached methyl group (-CH_3) of toluene can interact with another molecule. Self-associated toluene shows molecular association through the non-conventional C-H-π interactions (Fig. 2a). The interaction length of this association is approximately 3.300 Å, accompanied by a 0.001 Å increase in the C–H bond length.

DMSO-DMSO: DMSO molecules associate in chains with parallel dipole moments in their pure state, while neighbouring DMSO molecules from adjacent chains are oriented with anti-parallel dipole moments, as reported by Bertagnolli *et al.* [35] using X-ray and neutron scattering and confirmed by Vaisman & Berkowitz [36] using molecular dynamics simulation. In Fig. 2b, optimized geometry structure of DMSO dimer, both subunits are strongly associated due to highly polar S=O group. Two intermolecular H-bonds are formed between the two DMSO molecules of length 2.448 Å each. Here also the bond length r(S-O) increases by 0.009 Å in the donor molecule. Ali *et al.* [37] also reported the most stable structure of DMSO dimer has a similar well-fitted geometry.

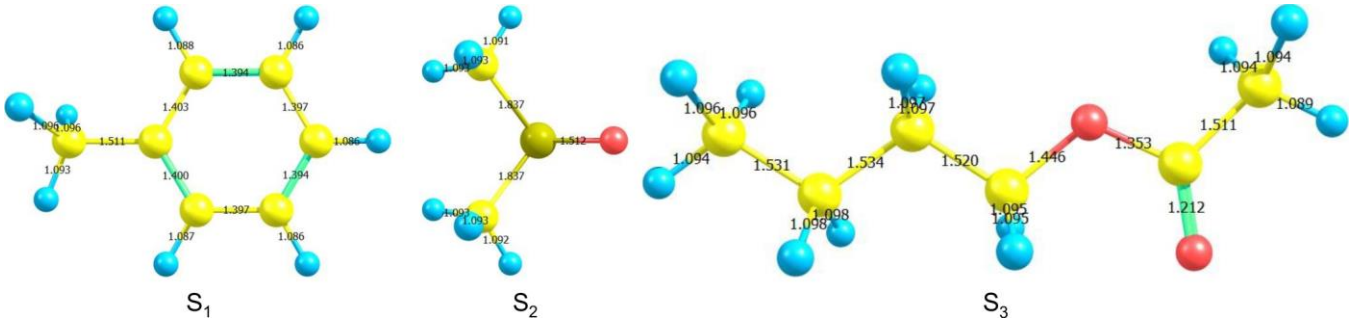

Fig. 1. Optimized geometry of (S_1) Tol monomer (S_2) DMSO monomer (S_3) BA monomer (distances in Å) obtained by DFT/B3LYP/6-311++G (d,p). The colour scheme- carbon: yellow, hydrogen: blue, oxygen: red & green: sulfur

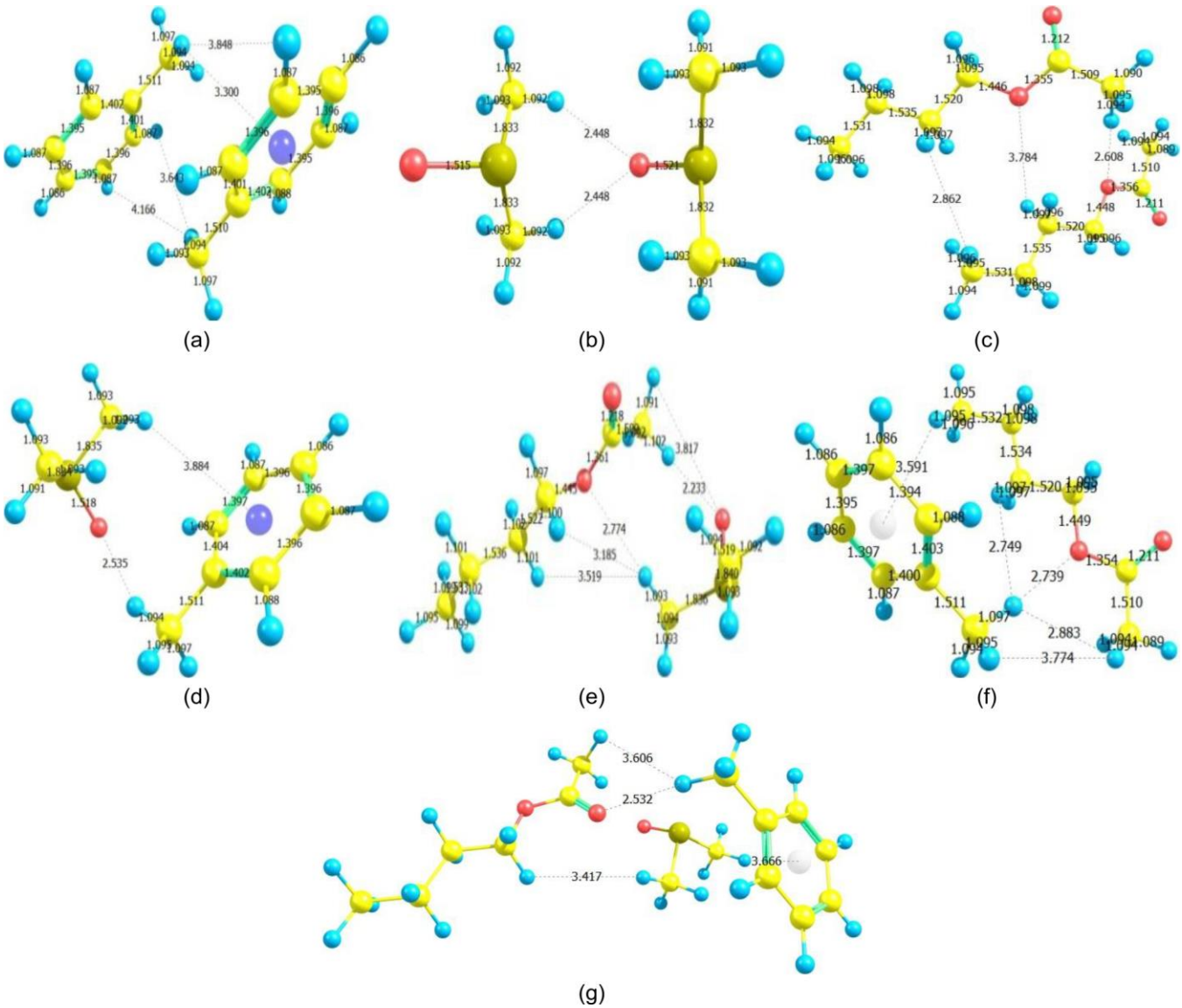

Fig. 2. Optimized geometry of (a) Tol dimer (b) DMSO dimer (c) BA dimer (d) Tol + DMSO, (e) DMSO + BA, (f) Tol + BA and (g) Tol + DMSO + BA complex (distances in Å) obtained by DFT/B3LYP/6-311++G (d,p). The color scheme- carbon: yellow, hydrogen: blue, oxygen: red & green: sulfur

BA-BA: In the butyl acetate dimer structure (Fig. 2c), the two intermolecular hydrogen bonding and a CH-C bonding take place between two subunits whose lengths are 2.608 Å, 3.784 Å and 2.862 Å, respectively. The bond length r(C2-O) is found to increases in both the subunits.

Tol + DMSO: The aromatic hydrocarbon molecules possess large quadrupole moment, which results an orientational order when mixed with other liquids [38,39]. This orientational order is thought of as a partial alignment of neighbouring segments or possibly of whole molecules. The oxygen atom

in DMSO carries a partial negative charge, which makes it a hydrogen bond acceptor but it can also act as a donor when interacting with certain molecules, especially water. In the optimized toluene and DMSO cluster (Fig. 2d), there exists the mutual dissociation of DMSO-DMSO molecule and association of Tol-Tol molecules resulting in subsequent formation of DMSO-Tol association. There is hydrogen bonding (>S=O ---C-H) interactions, between an acceptor oxygen atom of highly polar S=O group of DMSO and hydrogen atom of electron releasing group (-CH_3) of toluene molecules. The interaction length of this hydrogen bonding is about 2.535 Å. The bond length r(S-O) increases by 0.006 Å in DMSO and the bond length r(C-H) decreases by 0.002 Å in toluene. This type of hydrogen bonding interaction of (>S=O) group of DMSO is also observed in the binary mixture of DMSO + alkanol [38]. However, the hydrogen bonding group in DMSO-Tol is CH where as in DMSO alkanol it is OH.

DMSO + BA: In the optimized DMSO and butyl acetate structure, there exists a hydrogen bond interaction between the C-H hydrogen of DMSO and the C-C-O oxygen of butyl acetate (Fig. 2e). The interaction length of this interaction is about 2.774 Å and the bond length r(C_2-O) increases by 0.008 in butyl acetate.

BA + Tol: In the toluene and butyl acetate cluster (Fig. 2f), the C-H bond of butyl acetate takes a preferred geometry perpendicular to the π ring of toluene. The distance between the C-H of butyl acetate and the center of π ring of toluene is 3.591 Å. Also, the bond length of the r(C-H) of butyl acetate decreases by 0.001 Å. The shortening of this bond in butyl acetate shows that toluene and butyl acetate interact *via* CH-π interaction.

Tol + DMSO + BA: The stabilization of the Tol + DMSO + BA complex (Fig. 2g) takes place by different kinds of interaction between different moieties such as CH-π interaction between Tol and DMSO, OH bonding between toluene and butyl acetate, CH-C bonding between DMSO and butyl acetate with bond lengths 3.666 Å, 2.532 Å and 3.147 Å, respectively. The bond length r(C-O) and r(C-H) of butyl acetate increases by 0.007 Å and 0.001 Å, respectively. The space between toluene and butyl acetate molecule is the largest.

Molecular orbital and interaction energy analysis: For determining the kinetic stabilization and chemical activities of molecules and complexes, the study of the energy of HOMO, LUMO and the energy gap (ΔE) between them are the important parameters in quantum chemistry [40]. The orbital analysis of dimers and complexes done at wB97X-D level theory is summarized in Table-1. It is known that the orbital interaction exists between close orbitals in which the distance between orbital centers is usually less than 3.0 Å [41, 42]. The values of HOMO and LUMO suggest that orbital interaction is associated in all complexes with different amounts. On dimerization, the HOMO-LUMO energy gap decreases for all. The interaction energies which are determined by the supermolecular method [43] and the dipole moment of monomers, their dimers and complexes are summarized in Table-2. The total interaction energy (E_{total}) was calculated as the difference between the calculated energy of the dimer [E(AB)] and the sum of the calculated energies of monomers [E(A) and E(B)] as shown in eqn. 1:

$$E_{total} = E(AB) - [E(A) + E(B)] \quad (1)$$

The self-association of toluene shows the parallel orientation of rings with interaction energy -7.3982 Kcal/mol. The interaction energy of self-associated DMSO is -10.3506 Kcal/mol and the interaction energy of self-associated BA is -4.3567 Kcal/mol. So, it is much easier for DMSO to disrupt the self-association of toluene and self-association of butyl acetate, which results the formation of DMSO + Tol and DMSO + BA complex with stabilization energy of -23.944 Kcal/mol and -5.4141 Kcal/mol, respectively. DMSO dimer and BA dimer both are stabilized through weak intramolecular C-H---O hydrogen bonding.

Thus, the formation of (DMSO + Tol) and (BA + Tol) complexes are feasible through the breaking of weak non-covalent interactions present in dimer of DMSO and dimer of BA. As compared to interaction between DMSO and BA (DMSO + BA) (interaction energy = -5.4141 Kcal/mol), the interaction of toluene with DMSO (DMSO + Tol) and toluene with BA (BA + Tol) are more favourable as evident from the greater energy of interaction of about -23.9441 Kcal/mol and -26.4761 Kcal/mol, respectively. Functional wB97X-D includes dispersive interactions [44] due to which wB97X-D functional improves the interaction energy results qualitatively and also give greater interaction energies compared to the B3LYP, functional.

The interaction energy of the Tol + DMSO + BA ternary complex is –218.6649 Kcal/mol by wB97X-D level theory.

TABLE-1
HOMO-LUMO ENERGY AND ENERGY GAP VALUES OF DIMERS AND THEIR CLUSTERS WERE OBTAINED BY DFT WITH wB97X-D/6-311++G(d,p) LEVEL

Structure	wB97X-D			
	HOMO (a.u.)	LUMO (a.u.)	Energy gap (ΔE) (a.u.)	Energy gap (ΔE) (Kcal/mol)
Tol	-0.24772	-0.01723	-0.23049	-144.632475
DMSO	-0.3.1190	-0.12314	-0.42433	-266.267075
BA	-0.34964	-0.09711	-0.44675	-280.335625
Tol Dimer	-0.24334	-0.01953	-0.22381	-140.440775
DMSO Dimer	-0.28487	-011169	-0.39656	-248.841400
BA Dimer	-0.35087	-0.08353	-0.43440	-272.586000
Tol + DMSO	-0.30102	-0.07740	-0.37842	-237.458550
DMSO + BA	-0.30492	-0.09789	-0.40281	-252.763275
BA + Tol	-0.31258	-0.06963	-0.38221	-239.836775
Tol + DMSO + BA	-0.29204	-0.06846	-0.36050	-226.213750

TABLE-2
SINGLE POINT ENERGY AND DIPOLE MOMENT VALUES OF MONOMERS, THEIR DIMERS AND CLUSTERS OBTAINED BY DFT WITH B3LYP/6-311++G(d, p) AND wB97X-D/6-311++G(d,p) LEVEL AND THE INTERACTION ENERGIES OF THE COMPLEXES CALCULATED BY THE SUPER MOLECULAR METHOD

Structure	B3LYP				wB97X-D			
	Dipole moment (D)	Energy (a.u.)	Interaction energy (a.u.)	Interaction energy (Kcal/mol)	Dipole moment (D)	Energy (a.u.)	Interaction energy (a.u.)	Interaction energy (Kcal/mol)
Tol	0.4044	-271.638859	–	–	0.3994	-271.534525	–	–
DMSO	3.9315	-553.195519	–	–	4.0406	-553.126034	–	–
BA	2.0299	-386.351383	–	–	2.0661	-386.231280	–	–
Tol Dimer	0.0451	-543.287462	-0.009743	-6.1143	0.0474	-543.080840	-0.011790	-7.3982
DMSO Dimer	4.9090	-1106.401788	-0.010750	-6.7456	4.3498	-1106.268563	-0.016495	-10.3506
BA Dimer	2.1298	-772.704895	-0.002129	-0.0001	2.1473	-772.469503	-0.006943	-4.3567
Tol + DMSO	3.6489	-824.780973	-0.053405	33.5116	3.8063	-824.6222401	-0.038158	-23.9441
DMSO + BA	5.5681	-939.554282	-0.007380	-4.6309	5.7251	-939.365942	-0.008628	-5.4141
BA + Tol	1.9964	-657.932493	-0.057749	-36.2375	2.0118	-657.723612	-0.042193	-26.4761
Tol + DMSO + BA	2.1657	-1211.139847	-0.045914	-28.8110	2.2537	-1210.543369	-0.348470	-218.6649

Table-2 shows that there is increase in dipole moment for DMSO dimer and BA dimer due to H-bond formation between their clusters. The polarity of DMSO induces a dipole moment in Tol molecules and this induced dipole causes polarization of DMSO molecule, which results in overall decrease in dipole moment of DMSO (Table-2). It seems that the reverse dipole moment is induced by Tol in DMSO.

UV-Vis spectral analysis: The phenomena of charge transfer or redistribution of charge between different molecules was introduced by Mulliken and widely discussed by Foster to define a new type of adduct of different molecules. Molecular interaction exists between electron donors and acceptors and this often produce coloured charge transfer complexes and these charge transfer complexes absorb radiation in the UV and visible regions [45-48]. A shift in the spectral frequencies of the complexes is observed compared to the pure compounds, along with a decrease in absorbance. The experimental UV-Vis spectra of the mixture of toluene, DMSO with butyl acetate at different concentrations is shown in Fig. 3. It is observed that as the mole fraction of toluene increases, the spectra shift towards a longer wavelength.

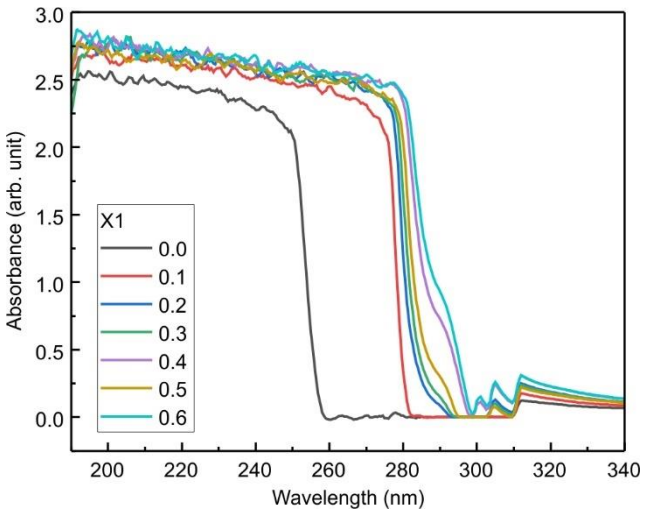

Fig. 3. Experimentally measured UV-Vis spectra of ternary mixture of Tol + DMSO + BA with increasing mole fraction of toluene from X_1 = 0.0 to 0.6

This red shift could be due to the higher π-electron density of toluene to the neighboring atoms or molecules by inductive effect and resonance effect. For X_1 = 0.0 to 0.4 and X_1 = 0.6, CH-C and OH interaction red shift while at 0.5, CH-π interaction causes blue shift in the absorbance spectra. The wavelength corresponding to the absorption maxima increases for all the concentrations which is due to the increasing conjugation in the mixture (increased mole fraction of toluene). With increasing concentration, the shift in wavelength of the absorbance maxima follows a uniform pattern. The main factor contributing to this uniformity is that the energy produced by the electron transition is directly proportional to the concentration of the solution.

FT-IR spectral studies: The experimental FT-IR spectroscopy precisely measures the properties of association, hydrogen bonding capability and to analyze the interaction among the components through the changes in band shifts and band shape. The change or shift in frequency (wavenumber) of the X-H stretch vibration in the H-bonding proton donor can be classified into red- shifted and blue-shifted X-H vibrations [49]. Red-shifted H-bonds are characteristic of the elongation of the H-X bond, which results a decrease in the frequency of the H-X stretching vibration and the increase in the IR intensity. On the other hand, blue-shifted H-bonds shows that H-X bond gets shorter with a subsequent increase in the H-X stretching frequency. Some researchers suggest that the shifts whether red or blue-shift of the H-X bond are due to the balance of electrostatic attractive and repulsive Pauli steric interactions at the equilibrium geometry [50]. Table-3 summarizes the spectral peak and vibrational bands of pure components taken from the literature [51-56]. The FT-IR spectra of pure compounds used in the present work and their ternary mixture at different mole fractions and the range of wavenumber are presented in Figs. 4a-f and reported in Table-4, respectively. The frequency ranges that depend on different vibrational bands are discussed as follows:

O-H stretching: Generally, the O-H stretching band due to the free O–H group appears as a sharp band at a higher frequency range of 3650-3590 cm^{-1}, however, the O–H stretching due to the intermolecular hydrogen bonding, which broadens the band and shifts its position to lower frequency is

TABLE-3
FT-IR SPECTRAL PEAK(S) AND VIBRATIONAL BANDS OF PURE COMPONENTS OF TOLUENE, DMSO, BUTYL ACETATE WERE TAKEN FROM THE LITERATURE [50-55]

Toluene		DMSO		Butyl acetate	
ν (cm^{-1})	Band	ν (cm^{-1})	Band	ν (cm^{-1})	Band
2891.7, 2894.1, 2873, 2862	CH stretching	1438, 1405	CH_3 stretching (asym)	3006	CH_3 stretching (asym)
2939.6, 3073.0, 2925, 2949, 2920	CH stretching	1310	CH_3 stretching (sym)	2968, 2961	CH_2 stretching (asym)
1617	C=C stretching	1075	SO stretching	1762	C=O stretching
1419.7, 1456.3, 1495	C-C stretching (aromatic)		-	1241, 1366	C-C-O stretching

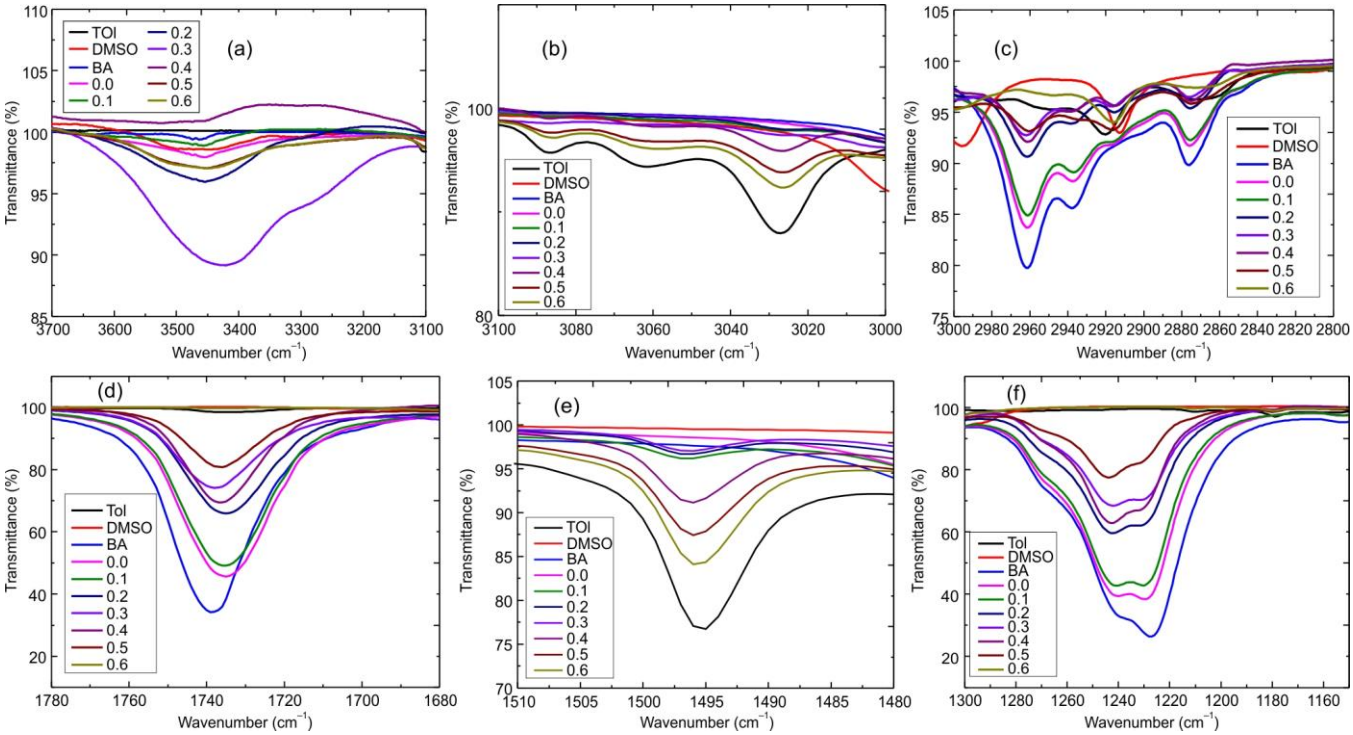

Fig. 4. FTIR spectra (a) (3700-3100 cm^{-1} wavelength range) (b) (3100-3000 cm^{-1} wavelength range) (c) (3000-2800 cm^{-1} wavelength range) (d) (1780-1680 cm^{-1} wavelength range) (e) (1510-1480 cm^{-1} wavelength rang and (f) (1300-1150 cm^{-1} wavelength range) of toluene, DMSO, butyl acetate and their mixture (The mole fraction of DMSO fixed at 0.4 and toluene (T) and butyl acetate (BA) varied from 0.0 to 0.6)

TABLE-4
FT-IR SPECTRAL PEAK(S) DETAILS OF WAVE NUMBER RANGE (3700-3100 cm^{-1}), (3100-2800 cm^{-1}), (1780-1680 cm^{-1}), (1510-1480 cm^{-1}) AND (1300-1150 cm^{-1}) OF TOLUENE, DMSO, BUTYL ACETATE AND THEIR MIXTURE

System	Peak (3700-3100) cm^{-1}		Peak (3100–2800) cm^{-1}						Peak (1780-1680) cm^{-1}		Peak (1510-1480) cm^{-1}		Peak (1300-1150) cm^{-1}	
	ν (cm^{-1})	T (%)	ν (cm^{-1})	T (%)	ν (cm^{-1})	T (%)	ν (cm^{-1})	T (%)	ν (cm^{-1})	T (%)	ν (cm^{-1})	T (%)	ν (cm^{-1})	T (%)
Toluene	–	–	3027	87.93	2950	95.28	2875	96.09			1496	76.70	–	–
DMSO	3472	98.60	–	–	2996	91.69	2913	93.63	–	–	–	–	–	–
Butyl acetate	3470	99.50	–	–	2962	79.76	2877	89.82	1739	34.24	–	–	1239	32.63
0	3455	97.96	–	–	2961	83.71	2876	91.70	1735	45.66	–	–	1240	39.38
0.1	3457	98.90	–	–	2961	84.90	2876	92.28	1735	49.09	1497	96.21	1240	42.72
0.2	3455	95.97	–	–	2961	90.64	2876	95.39	1735	65.97	1497	94.68	1242	59.63
0.3	3424	89.18	–	–	2962	92.74	2876	96.12	1738	74.16	1497	97.04	1242	68.41
0.4	3455	100.90	3027	95.89	2961	92.10	2876	96.12	1736	69.42	1496	91.12	1243	62.81
0.5	3451	97.07	3027	93.82	2961	93.16	2876	95.83	1736	80.84	1496	87.40	1243	77.68
0.6	3451	97.07	3026	92.37	–	–	2865	97.48	–	–	1496	84.08	–	–

found in the range 3550-3200 cm^{-1} [57]. Fig. 4a shows the FT-IR spectrum of pure components and their ternary mixture over the entire range of concentration and in the wavenumber range of (3800-3100 cm^{-1}). At X_1 = 0.0 the O-H stretching band lies at 3455 cm^{-1} with 97.96% transmittance (Table-4). As the concentration of toluene increases in the mixture

broadening of peaks takes place. At X_1 = 0.6 mole fraction a broad O-H stretching band lies at a lower frequency of 3451 cm^{-1} with 97.07% transmittance. This indicates that intermolecular hydrogen bonding exists in the mixture. It is a well-known fact that the hydrogen bonding formation lowers the wavenumber or frequency of OH stretching vibration and hence a broader band appears at a lower frequency as compared to the free OH group [58]. At 0.3 mole fraction of toluene, the intermolecular hydrogen bonding increases which is evident by further broadening of the O-H stretching band and shifts in frequency to the lower wave number of about 3424 cm^{-1} with considerable increase in intensity (89.14%). It is well established that a sharp and less intense band is observed at a higher frequency due to less extensive hydrogen bonding but extensive hydrogen bonding is responsible for a broad band at a lower frequency [59]. At 0.4 mole fraction, 100 % transmittance indicates the absence of spectral peak of the O-H bond.

Aromatic C-H stretching: The C-H stretching band of toluene shows a peak at 3027 cm^{-1} (Fig. 4b) in the range 3100-3000 cm^{-1}. At lower concentrations of toluene no shift in the CH bond exists in the mixture. However, a higher concentration of toluene at 0.6 shows a very small shift towards lower wave number (red shift) of 1 cm^{-1} with increased transmittance. This can be attributed to the formation of new hydrogen bond between toluene and highly polar DMSO. The theoretical analysis further supports the formation of hydrogen bonding within the mixture. The C–H stretching vibrations of DMSO and butyl acetate are observed in the range of 3000-2800 cm^{-1} (Fig. 4c), with the characteristic peaks appearing at 2996 cm^{-1} for DMSO and 2962 cm^{-1} for butyl acetate. A visible red shift in the C–H stretching frequencies indicates an elongation of the C–H bond in the mixture, which corroborates the theoretical prediction of CH···O interactions. These interactions are primarily responsible for the observed red shift, confirming the presence of weak hydrogen bonding between the components.

C=O stretching: From Fig. 4d, the C=O stretching band of BA shows a peak at 1739 cm^{-1} with 34.24% transmittance. In the mixture from 0.0 to 0.6, the bond length of C=O in butyl acetate get increased and there is shift towards a lower wavenumber with increased transmittance. This suggests that as compared to butyl acetate the interaction strength in the mixture is strong.

Aromatic C-C stretching: The aromatic C-C stretching band of toluene shows a peak at 1496 cm^{-1} with 77.04% transmittance (Fig. 4e). In the mixture, the aromatic C-C vibration of toluene shifts towards higher wave number. This indicates the shortening of C-C bond length which is due to the interaction between toluene gets strengthened in the mixture and also leads to a blue shift of absorption frequency. The similar observations of the blue shift of C-C stretching frequency is reported by Li *et al.* [59] for the pyridine + water complex and Hema *et al.* [60] for the *n*-hexane + ethanol + benzene mixture. The absorption intensity of IR spectra depends on molecular dipole moment [61,62]. An increase in the intensity of aromatic C-C stretching with increasing mole fraction shows the increase in molecular dipole moment in a polar (DMSO) environment.

C-O stretching: From Fig. 4f, the C-O stretching band of BA is observed at 1239 cm^{-1} with 32.63% transmittance. In the mixture there exists a hydrogen bonding interaction between the aliphatic C-H hydrogen of DMSO and the C-C-O oxygen, then the flow of electron from the donor oxygen towards the C-H hydrogen should result in red and blue shift in the C-H and C-O stretching frequencies. These shifts are also supported by the theoretical result of OH interaction between DMSO and butyl acetate (Fig. 4e). Therefore, the red shift in the aliphatic CH stretching may be coupled with the blue-shifted C-C-O stretching bonds to conclude that classical C-H-O-C-C hydrogen bond have been formed between DMSO and butyl acetate. A small shift of about 1 cm^{-1} in C-C-O stretching bands in the mixture suggests that this H-bond may be very weak. A similar observation of blue shift of C-C-O stretching frequency is reported by Arivazhagan *et al.* [63] for benzene + methyl acrylate.

Conclusion

In present investigation, the study of non-covalent interaction between toluene, DMSO and butyl acetate is analyzed through DFT, UV-Vis and FT-IR studies. The presence of other molecules is responsible for the change in electron cloud distribution and hence the deformation of molecular orbitals and shifts in energy levels of the molecules takes place. These orbital deformations also lead to several other changes such as change in bond length, dipole moment and bond order variation. Quantum mechanical calculations on dimers and complexes provide significant information of such variation and based on these qualitative details, we can ascertain the type and nature of the interaction between the molecules. Using DFT theory, we analyzed the optimized structure of the individual molecules, their dimers and complexes. Theoretical calculations on the optimized dimers and complexes show different type of possible molecular interaction between unlike molecules. DMSO dimer is self-associated through conventional H bonding. In toluene + DMSO + butyl acetate ternary mixture, three types of interaction, *i.e.* CH-π interaction, CH-C interaction and H-bonding, are present with interaction energy 7.39-26.47 kcal/mol, 4.35-7.39 kcal/mol and 5.41-26.47 kcal/mol, respectively. So, the order of interaction energies is CH-C < H-bonding < CH-π. On dimerization, the HOMO-LUMO energy gap decreases for toluene, DMSO, butyl acetate due to the intermolecular interaction. Specific interaction changes the HOMO- LUMO energy gap and also changes the structure of HOMO orbital and hence affects the absorption spectra. CH-C and OH interaction between DMSO and butyl acetate causes red shift while at 0.5, CH-π interaction between toluene and DMSO causes blue shift in the absorption spectra. Since different interactions between the molecules have their own effect on the molecular absorption spectra, therefore the presence of a liquid mixture rather than a single compound results in the absorption spectra that are broader with several peaks. The OH, CH, C=O, C-C stretching vibration bands shift towards the lower wavenumber in the ternary mixture. The shifts in IR frequencies are due to the molecular interaction between unlike molecules. The change in band intensity and shift in IR frequencies strongly supports the existence of weak interaction in the ternary liquid mixture.

ACKNOWLEDGEMENTS

A special thanks to Prof. Dr. Nanda Gopal Sahoo, In-Charge PRS-Nanoscience & Nanotechnology Centre, Depart-

ment of Chemistry, DSB Campus, Kumaun University, Nainital for UV & FT-IR instrument facilities.

CONFLICT OF INTEREST

The authors declare that there is no conflict of interests regarding the publication of this article.

REFERENCES

1. B. García, R. Alcalde, J.M. Leal and J.S. Matos, *J. Chem. Soc., Faraday Trans.*, **93**, 1115 (1997); https://doi.org/10.1039/a607876a
2. O.A. El Seoud, S. Possidonio and N.I. Malek, *Liquids*, **4**, 73 (2024); https://doi.org/10.3390/liquids4010003
3. A. Mchaweh, A. Alsaygh, K. Nasrifar and M. Moshfeghian, *Fluid Phase Equilib.*, **224**, 157 (2004); https://doi.org/10.1016/j.fluid.2004.06.054
4. A.S. Bahadur, M.C.S. Subha and K.C. Rao, *J. Pure Appl. Ultrason.*, **23**, 26 (2001).
5. P.S. Rao, M.C.S. Subha and G.N. Swamy, *Acustica*, **83**, 155 (1997).
6. M.B. Ewing, B.J. Levien, K.N. Marsh and R.H. Stokes, *J. Chem. Thermodyn.*, **2**, 689 (1970); https://doi.org/10.1016/0021-9614(70)90044-3
7. A. Ali, A.K. Nain and M. Kamil, *Thermochim. Acta*, **274**, 209 (1996); https://doi.org/10.1016/0040-6031(95)02719-X
8. A. Rohman and A. Windarsih, *Int. J. Mol. Sci*., **21**, 5155 (2020); https://doi.org/10.3390/ijms21145155
9. Pankaj and C. Sharma, *Ultrasonics*, **29**, 344 (1991); https://doi.org/10.1016/0041-624X(91)90033-5
10. S. Velmurugan, T.K. Nambinarayanan, R.A. Srinivasa and B. Krishnan, *Indian J. Phys.*, **618**, 105 (1987).
11. J.M.G. Cowie, *J. Polym. Sci. Part C Polym. Symp.*, **23**, 267 (1968); https://doi.org/10.1002/polc.5070230133
12. A. Pal and G. Das, *J. Pure Appl. Ultrasonic*, **21**, 9 (1990).
13. C. Di Mino, A. J. Clancy, A. Sella, C. A. Howard, T. F. Headen, A. G. Seel, and N.T. Skipper, *J. Phys. Chem. B*, **127**, 1884 (2023); https://doi.org/10.1021/acs.jpcb.2c07155
14. M. Šimunková and M. Malček, *Acta Chim. Slov.*, **13**, 38 (2020); https://doi.org/10.2478/acs-2020-0022
15. P. Arya, T. Bhatt, H. Arya, C.C. Dhondiyal and M. Rana, *Chem. Africa*, **7**, 1033 (2024); https://doi.org/10.1007/s42250-023-00779-0
16. G. Arul and L. Palaniappan, *Indian J. Pure Appl. Phys.*, **39**, 561 (2001).
17. S. Thirumaran and J.E. Jayakumar, *Indian J. Pure Appl. Phys.*, **47**, 265 (2009).
18. S. Tsuzuki, K. Honda, T. Uchimaru, M. Mikami and K. Tanabe, *J. Phys. Chem. A*, **106**, 4423 (2002); https://doi.org/10.1021/jp013723t
19. H. Chen, X. Xu, S. Gong, Y. Zhou and Z. Wang, *J. Mol. Liq*., **313**, 113542 (2020); https://doi.org/10.1016/j.molliq.2020.113542
20. K. Umasivakami, S. Vaideeswaran and V. Rose, *J. Serb. Chem. Soc.*, **83**, 1131 (2018); https://doi.org/10.2298/JSC170829056U
21. H. Chen, Z. Wang, X. Xu, S. Gong and Y. Zhou, *Phys. Chem. Chem. Phys.*, **23**, 13300 (2021); https://doi.org/10.1039/D1CP00874A
22. L.A. Curtiss, K. Raghavachari, G.W. Trucks and J.A. Pople, *J. Chem. Phys.*, **94**, 7221 (1991); https://doi.org/10.1063/1.460205
23. S. Jeff, *J. Chem. Pharm. Res*., **16**, 95 (2024); https://doi.org/10.37532/0975-7384.2024.16(1).095
24. R. Vargas, J. Garza and A. Martínez, *J. Mex. Chem. Soc.*, **68**, 970 (2024); https://doi.org/10.29356/jmcs.v68i4.2306
25. Hema, T. Bhatt, T. Pant, C.C. Dhondiyal, M. Rana, P. Chowdhury, G. C. Joshi, P. Arya and H. Tiwari, *J. Mol. Model.*, **26**, 268 (2020); https://doi.org/10.1007/s00894-020-04533-y
26. Y. Zhao and D.G. Truhlar, *J. Chem. Theory Comput*., **1**, 415 (2005); https://doi.org/10.1021/ct049851d
27. S. Scheiner, *J. Phys. Chem. B*, **110**, 18670 (2006); https://doi.org/10.1021/jp063225q
28. R.O. Jones, *Rev. Mod. Phys.*, **87**, 897 (2015); https://doi.org/10.1103/RevModPhys.87.897
29. M.J. Frisch, G.W. Trucks, H.B. Schlegel, G.E. Scuseria, M.A. Robb, J.R. Cheeseman, G. Scalmani, V. Barone, B. Mennucci, G.A. Petersson, H. Nakatsuji, M. Caricato, X. Li, H.P. Hratchian, A.F. Izmaylov, J. Bloino, G. Zheng, J.L. Sonnenberg, M. Hada, M. Ehara, K. Toyota, R. Fukuda, J. Hasegawa, M. Ishida, T. Nakajima, Y. Honda, O. Kitao, H. Nakai, T. Vreven, J.A. Montgomery, J.J.E. Peralta, F. Ogliaro, M. Bearpark, J.J. Heyd, E. Brothers, K.N. Kudin, V.N. Staroverov, T. Keith, R. Kobayashi, J. Normand, K. Raghavachari, A. Rendell, J.C. Burant, S.S. Iyengar, J. Tomasi, M. Cossi, N. Rega, J.M. Millam, M. Klene, J.E. Knox, J.B. Cross, V. Bakken, C. Adamo, J. Jaramillo, R. Gomperts, R.E. Stratmann, O. Yazyev, A.J. Austin, R. Cammi, C. Pomelli, J.W. Ochterski, R.L. Martin, K. Morokuma, V.G. Zakrzewski, G.A. Voth, P. Salvador, J.J. Dannenberg, S. Dapprich, A.D. Daniels, O. Farkas, J.B. Foresman, J.V. Ortiz, J. Cioslowski and D.J. Fox, Gaussian 09, Revision E.01, Gaussian, Inc., Wallingford CT (2013).
30. M.D. Hanwell, D.E. Curtis, D.C. Lonie, T. Vandermeersch, E. Zurek and G.R. Hutchison, *J. Cheminform.*, **4**, 17 (2012); https://doi.org/10.1186/1758-2946-4-17
31. A.D. Becke, *Phys. Rev. A Gen. Phys.*, **38**, 3098 (1988); https://doi.org/10.1103/PhysRevA.38.3098
32. C. Lee, W. Yang and R.G. Parr, *Phys. Rev. B Condens. Matter*, **37**, 785 (1988); https://doi.org/10.1103/PhysRevB.37.785
33. L. Sobczyk, S.J. Grabowski and T.M. Krygowski, *Chem. Rev.*, **105**, 3513 (2005); https://doi.org/10.1021/cr030083c
34. https://www.chemcraftprog.com
35. H. Bertagnolli, E. Schultz and P. Chieux, *Ber. Bunsenges. Phys. Chem*, **93**, 88 (1989); https://doi.org/10.1002/bbpc.19890930117
36. L.I. Vaisman and M.L. Berkowitz, *J. Am. Chem. Soc.*, **114**, 7889 (1992); https://doi.org/10.1021/ja00046a038
37. A. Ali, S. Hyder and M. Tariq, *Int. J. Thermophys.*, **26**, 1537 (2005); https://doi.org/10.1007/s10765-005-8102-9
38. D. Patterson, *J. Solution Chem.*, **23**, 105 (1994); https://doi.org/10.1007/BF00973540
39. M.I. Sancho, M.C. Almandoz, S.E. Blanco and E.A. Castro, *Int. J. Mol. Sci*., **12**, 8895 (2011); https://doi.org/10.3390/ijms12128895
40. J. Li and R.Q. Zhang, *Sci. Rep.*, **6**, 22304 (2016); https://doi.org/10.1038/srep22304
41. J. Li and R.Q. Zhang, *Phys. Chem. Chem. Phys.*, **17**, 29489 (2015); https://doi.org/10.1039/C5CP04684J
42. S. Tsuzuki and T. Uchimaru, *Curr. Org. Chem.*, **10**, 745 (2006); https://doi.org/10.2174/138527206776818937
43. Hema, T. Bhatt, T. Pant, C.C. Dhondiyal and H. Tiwari, *Indian J. Chem.*, **60A**,1072 (2021).
44. R.S. Mulliken, *J. Am. Chem. Soc.*, **72**, 600 (1950); https://doi.org/10.1021/ja01157a151
45. R.S. Mulliken and W.B. Pearson, Molecular Complexes, Wiley Publishers: New York (1969).
46. R. Foster, Charge-transfer Complexes, Academic Press: London, p. 387 (1969).
47. Z.Y. Li, H.L. Wang, T.J. He, F.C. Liu and D.M. Chen, *J. Mol. Struct. THEOCHEM*, **778**, 69 (2006); https://doi.org/10.1016/j.theochem.2006.08.048
48. P. Hobza and Z. Havlas, *Chem. Rev.*, **100**, 4253 (2000); https://doi.org/10.1021/cr990050q
49. X. Li, L. Liu and H.B. Schlegel, *J. Am. Chem. Soc.*, **124**, 9639 (2002); https://doi.org/10.1021/ja020213j
50. G.E. Douberly, A.M. Ricks, P.V.R. Schleyer and M.A. Duncan, *J. Phys. Chem. A*, **112**, 4869 (2008); https://doi.org/10.1021/jp802020n
51. R. Knaanie, J. Šebek, M. Tsuge, N. Myllys, L. Khriachtchev, M. Räsänen, B. Albee, E.O. Potma and R.B. Gerber, *J. Phys. Chem. A*, **120**, 3380 (2016); https://doi.org/10.1021/acs.jpca.6b01604
52. J. Datka, *J. Chem. Soc., Faraday Trans. I*, **77**, 511 (1981); https://doi.org/10.1039/F19817700511
53. N. Mozhzhukhina, L.P. Méndez De Leo and E.J. Calvo, *J. Phys. Chem. C*, **117**, 18375 (2013); https://doi.org/10.1021/jp407221c

54. S. Kumar and L. Guganathan, *J. Emerg. Technol. Innov. Res.*, **5**, 544 (2018).
55. Omni-Cell Transmission) AN20-03, Liquid film FT-IR analysis of esterification reaction products in the Omni-Cell Specac Ltd. (2022).
56. J.R. Dyer, Applications of Absorption Spectroscopy of Organic Compounds, Prentice-Hall of India, New Delhi, edn 4 (1978).
57. Hema, T. Bhatt, P. Arya, C.C. Dhondiyal, H. Tiwari and K. Devlal, *Struct. Chem.*, **33**, 207 (2022); https://doi.org/10.1007/s11224-021-01832-9
58. A. Awasthi and J.P. Shukla, *Ultrasonics*, **41**, 477 (2003); https://doi.org/10.1016/S0041-624X(03)00127-6
59. A.Y. Li, H.B. Ji and L.J. Cao, *J. Chem. Phys.*, **131**, 164305 (2009); https://doi.org/10.1063/1.3251123
60. Hema and T. Bhatt, *Mater. Today*, **47**, 1590 (2021); https://doi.org/10.1016/j.matpr.2021.04.264
61. J.S. Bader and B.J. Berne, *J. Chem. Phys.*, **100**, 8359 (1994); https://doi.org/10.1063/1.466780
62. R. Ramírez, T. López-Ciudad, P. Kumar P and D. Marx, *J. Chem. Phys.*, **121**, 3973 (2004); https://doi.org/10.1063/1.1774986
63. G. Arivazhagan, A. Elangovan, R. Shanmugam, R. Vijayalakshmi and N.K. Karthick, *J. Mol. Liq.*, **214**, 357 (2016); https://doi.org/10.1016/j.molliq.2015.10.062